Engineering Science and Technology, an International Journal 48 (2023) 101562

Contents lists available at ScienceDirect

Engineering Science and Technology, an International Journal

journal homepage: www.elsevier.com/locate/jestch

A quasi-analytical prediction method for gear load-independent power losses for shroud approaching

X. Zhu, J.N. Bian, Y. Dai *

College of Mechanical and Electrical Engineering, Central South University, Changsha 410083, China

ARTICLE INFO

Keywords:
Shrouded meshed gears
Squeezing/pocketing behavior
Windage losses
Load-independent losses
Swept volume

ABSTRACT

To limit the adverse effect of the fluid pressure field in high-speed gearing systems, especially for the main reducer of helicopters, shrouds usually adopted to enclose and approaches the high-speed gears will play a vital role in the windage and pumping power losses in axial and radial directions. To better explore and predict the total load-independent losses, this paper proposes an improved quasi-analytical method to quantify the power losses caused by the windage and pumping effects, considering the gear pump characteristics with the compressibility of the air or air-oil mixture. The theoretical calculations using the improved model are then compared with experimental results in the open literature. Leveraging the swept volume of the gear pump, the squeezing/pocketing behavior of the fluids in the tooth space can get a better understanding as the shroud approaches the gear pair.

1. Introduction

Gear system is one of the key components of aero engines and helicopter transmissions, where the rotating speed of the input stage is up to 20,000 r/min, accompanied by greater power losses. A huger energy dissipation implies a stricter and more rigorous requirement of onboard lubrication and cooling system and endurance mileage. Regarding the high-speed gear transmission, load-independent power losses dominating the total losses can easily reach 2–3 % of the transmission power [1–2]. In general, gear load-independent losses mainly include windage losses, churning losses, and pumping losses, windage power losses have contributed most to the total losses above 90–120 m/s tip tangential speeds [3]. Once the pitch velocity exceeds 127 m/s, the pumping power losses are also seen to be a significant part [4]. Due to the gear windage and churning losses approximately proportional to the third power of the rotating speed, the sum of these two losses is more than 50 % of the total energy dissipation of the gear system as the speed exceeding 100 m/s [5]. Thereby, shrouds are commonly adopted to limit these independent losses and improve the efficacy. Indeed, it is just what this paper tries to deal with the prediction of the power losses when the shroud approaches the gear pair.

Past research has been carried out to model the windage power losses of different kinds of gears. Diab et al. [6] proposed two quasi-analytical theoretical models to estimate the windage drag losses of an isolated single spur gear, detailly characterizing the drag moment of the fluid flow on the gear faces and inside the teeth. The theoretical method in Seetharaman and Kahraman [7–8] is similar, which is based on boundary layer theory to predict the windage losses as the sum of the loss on the faces and teeth space, this method is also applied to the case of splash lubrication [9]. Based on these, Zhu et al. [10–11] developed the theoretical and calculating models of windage losses for a single spiral bevel gear, presented as the sets of the toe/heel and the teeth. In general, different types of load-independent losses can be added up to quantify the total losses. Ruzek et al. [12–13] explored and determined the total losses of the no-meshing spur gear pair are approximately equal to the sum of the individual gear, the same conclusion is reached by Dai et al. [14]. Considering the windage effect, the total independent power losses of a splash-lubricated spiral bevel gear are effectively estimated [15–17], so is a splash and oil jet-lubricated orthogonal face gear [18–19].

Meanwhile, some researchers tried to model and estimate the gear pumping power losses. Pumping losses, namely the squeezing/pocketing power losses, are attached to the physical phenomenon of trapping and releasing the air or air-oil mixture in the given tooth interspace when the gears proceed through mesh [20–23]. Using the equation of continuity and energy, Daib et al. [24] used Euler's prediction and Newton-Raphson correction method to calculate the pressure distributions in a mesh cycle, verified by experimental data measured by the pressure

* Corresponding author.
E-mail address: 210143@csu.edu.cn (Y. Dai).

https://doi.org/10.1016/j.jestch.2023.101562
Received 5 April 2023; Received in revised form 21 September 2023; Accepted 23 October 2023
Available online 4 November 2023

sensors implanted under the gear surfaces, then determined the mean value of the pumping losses. Further leveraging the equation of momentum, Seetharaman and Kahraman [8,25] obtained the velocity distributions in a mesh cycle for the estimation of the resulting pumping losses, the results indicated that the pitch line velocity is the most powerful force driving these velocities and power losses, in addition, the velocities and pressures at the end is slightly lower than that at the backlash. A shroud has been recognized as an effective tool to mitigate windage power losses. Gorla et al. [26] replaced the air or air-oil mixture with oil to investigate the influence of geometrical and working parameters on the total power losses subjected to windage and pumping effects for a meshed gear pair in power transmissions. However, its advantageous effect may be offset for a shrouded meshed gear pair due to the squeezing/pocketing behavior in the vicinity of mesh, the related research reported by Delgado and Hurrell [27]. Meanwhile, Hurrell and Sawicki [4,28] also explored the squeezing/pocketing phenomenon of the meshed gears with a shroud by introducing the swept volume of the gear pump.

Benefiting from CFD techniques [29–31], the load-independent losses have been widely and systematically concerned, including windage [32–34], churning [35–38] and impacting phenomena [18,39–40]. Although there still exist some defects in modeling the gear meshing due to the compression and expansion of the very small cavity and contact of the gear pair in all time, Al et al. [41] conducted a 2D CFD study to explore the pressure change on the gear teeth during the mesh cycle by using several meshed teeth instead of a meshed gear pair, the numerical results agree well with experiments by Diab et al. [24]. Regarding the fluid flow to be isothermal and incompressible, Burberi et al. [23] exploited a dynamic mesh dealing with the meshed gear not in contact to investigate the meshed spinning gear pair partly submerged in an oil bath. Hurrell and Sawicki [4] adopted ASNSY CFX to simulate the engagement of the shrouded gears, and obtained the swept volume and mesh pressure of the gears in different configurations.

Making a better sense of load-independent losses of the shrouded gears is relatively scarce, especially for the shroud closely approaches the gears. Therefore, this paper presents a quasi-analytical method to deal with the prediction of the load-independent losses of the tightly shrouded meshed gears, considering the windage and pumping effects. Then, based on the volumetric change in the processes of compression and expansion of the given cavity and subsonic compressible flow characteristic, this theoretical calculation model is improved and then compared with experimental findings.

2. Quasi-analytical relationship

2.1. Description of the compression-expansion behavior

For a tooth of the pinion and the conjugate tooth of the gear, the evolution process of the compression-expansion behavior for the space tooth is depicted in Fig. 1. Points K_1 and K_2 represent the entry and exit points of the top of the pinion entering and exiting the tooth space of the gear. The volume of the tooth space experience from the single-teeth meshing (from point S_1 to point D_1), double-teeth meshing (from point D_1 to point D_2) to single-teeth meshing (from point D_2 to point S_2) processes, when the contact points changing from point S_1 (i.e., the top of the gear approaches the root of the pinion tooth) to S_2 (i.e., the top of the pinion reaches the gear dedendum), along with the volume first decreasing and then increasing, it means that the air or the air-oil mixture expelled from or sucked into the tooth space. Due to the gear engagement, the air or the air-oil mixture is blocked in the tooth space,

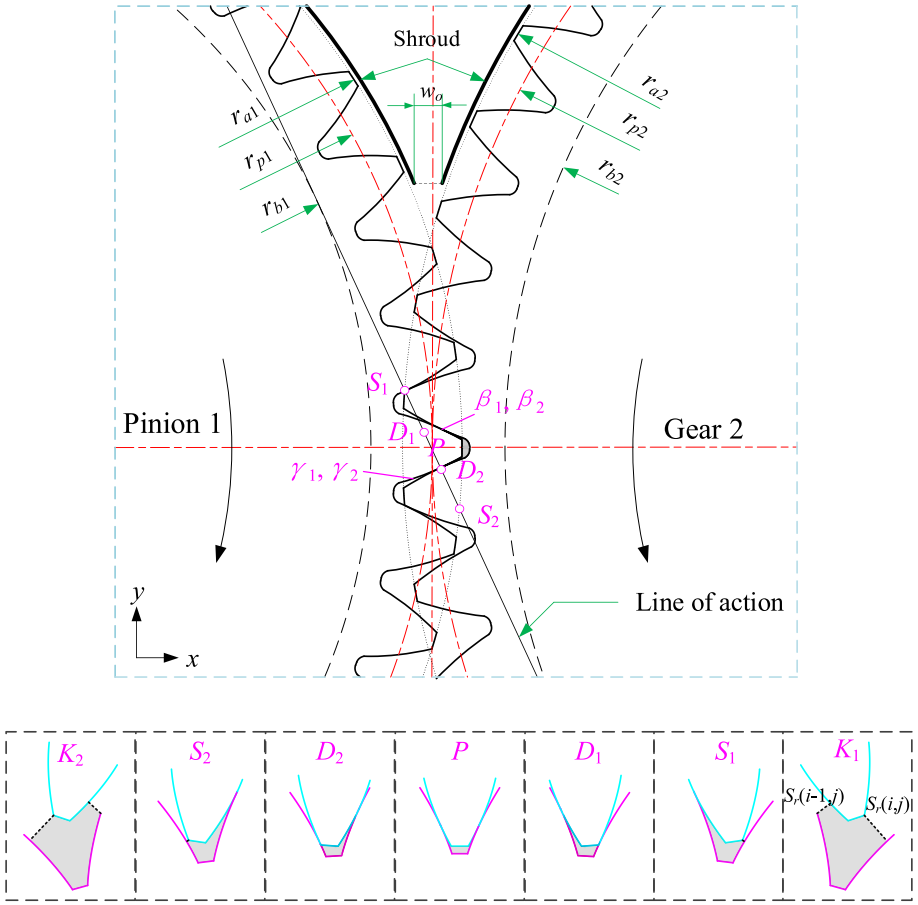

Fig. 1. Shrouded gear pair during the meshing.

causing variations in fluid density, pressure and temperature. This behavior mainly depends on the attributes of the air or the air-oil mixture (density, viscosity, etc.), gear geometry and operating parameters, the sonic or non-sonic conditions of the flow, the ambient pressure and temperature.

The involute tooth profile function of the pinion is presented based on the cartesian coordinate system as illustrated in Fig. 1, with the origin at the center of the pinion, expressed as:

$$\begin{bmatrix} x_0 \\ y_0 \end{bmatrix} = \begin{pmatrix} \cos(\pi/z_1) & \mp\sin(\pi/z_1) \\ \pm\sin(\pi/z_1) & \cos(\pi/z_1) \end{pmatrix} \begin{bmatrix} r_{b1}[\cos(\theta_{os1}+\theta_{ks1})+\theta_{ks1}\sin(\theta_{os1}+\theta_{ks1})] \\ \pm r_{b1}[\sin(\theta_{os1}+\theta_{ks1})-\theta_{ks1}\cos(\theta_{os1}+\theta_{ks1})] \end{bmatrix}, k = (\beta_1, \gamma_1) \quad (1)$$

and

$$\theta_{ks} = \tan\alpha_i \alpha_i \in [0, \arccos(r_b/r_a)]$$

$$\theta_{os} = \pi/2z - inv\alpha_p$$

The involute tooth profile function of the gear is then expressed as:

$$\begin{bmatrix} X_0 \\ Y_0 \end{bmatrix} = \begin{bmatrix} -r_{b2}[\cos(\theta_{os2}+\theta_{ks2})+\theta_{ks2}\sin(\theta_{os2}+\theta_{ks2})]-(r_{p1}+r_{p2}) \\ \mp r_{b2}[\sin(\theta_{os2}+\theta_{ks2})-\theta_{ks2}\cos(\theta_{os2}+\theta_{ks2})] \end{bmatrix}, k = (\beta_2, \gamma_2) \quad (2)$$

where r_a, r_b is the tip and base radius of the gears, θ_{os} denotes the angle parameter of the intersection point of involute and base circle, θ_{ks} represents the tooth surface parameter, α_i is the pressure angle at an arbitrary point, α_p denotes the pressure angle on pitch circle, subscript $_{1,2}$ represents the pinion and the gear, respectively.

After the pinion's arbitrary angle revolving, the profile function of these given teeth is obtained. For the pinion:

$$\begin{bmatrix} x \\ y \end{bmatrix} = \begin{pmatrix} \cos(\theta) & -\sin(\theta) \\ \sin(\theta) & \cos(\theta) \end{pmatrix} \begin{bmatrix} x_0 \\ y_0 \end{bmatrix} \quad (3)$$

and

$$\begin{bmatrix} X \\ Y \end{bmatrix} = \begin{pmatrix} \cos(\frac{z_1}{z_2}\theta) & \sin(\frac{z_1}{z_2}\theta) \\ -\sin(\frac{z_1}{z_2}\theta) & \cos(\frac{z_1}{z_2}\theta) \end{pmatrix} \begin{bmatrix} r_{p1}+r_{p2} \\ 0 \end{bmatrix} + \begin{pmatrix} -\cos(\frac{z_1}{z_2}\theta) & -\sin(\frac{z_1}{z_2}\theta) \\ \sin(\frac{z_1}{z_2}\theta) & -\cos(\frac{z_1}{z_2}\theta) \end{pmatrix} \begin{bmatrix} X_o \\ Y_o \end{bmatrix} + \begin{bmatrix} X_o \\ Y_o \end{bmatrix} \quad (4)$$

2.2. Calculation of the gear load-independent losses

According to the study of Ruzek et. al [12] and Dai et. al [14], the windage power losses of the no-meshing gear pair are the sum of the single individual gear. When a shroud approaches the spur gear pair (see Fig. 2), the resulting load-independent power losses can be regarded as the sum of the windage losses on the faces of the individual spur gears and the pumping losses at the gear backlash, expressed as:

$$P_{all} = P_{wind-1} + P_{wind-2} + P_{pump} \quad (5)$$

where P_{all} is the total resulting load-independent losses. P_{wind} and P_{pump} represent the power losses caused by the windage and squeezing/pocketing behavior, respectively. Subscript $_{1,2}$ denotes the driving and driven gears.

2.2.1. Windage losses

According to the quasi-analytical physical model proposed by Diab et al. [6], the windage losses of an isolated spur gear with or without a shroud can be determined as

$$P_{wind} = \frac{1}{2} C_w \rho \omega^3 r_p^5 \quad (6)$$

with: $C_w = C_f + C_t$. C_w, C_f, C_t is the dimensionless coefficient of the total moment, the moment on the front/rear faces, and the moment at the tooth space. ρ is the density of air or air-oil mixture surrounding the spinning gear. ω is the gear angular velocity. R_p connotes the pitch radius.

The dimensionless coefficient C_f is relevant to the flow regime, after combining the laminar and turbulent flows, then:

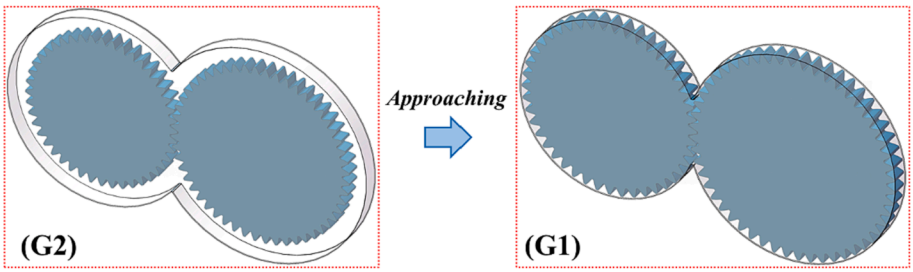

Fig. 2. A Shroud approaches the gear pair.

$$C_f = \underbrace{\frac{2n_L\pi}{5-2m_L}\frac{1}{Re^{*m_L}}\left(\frac{R^*}{r_p}\right)^5}_{\text{Laminar zone}} + \underbrace{\frac{2n_T\pi}{5-2m_T}\left[\frac{1}{Re^{m_T}} - \frac{1}{Re^{*m_T}}\left(\frac{R^*}{r_p}\right)^5\right]}_{\text{Turbulent zone}} \tag{7}$$

where n, m is the flow coefficients of the flow regime. Subscript $_{L,T}$ denotes the laminar and turbulent flows. Re* is the critical Reynolds number, with Re* $= 3 \times 10^5$. R^* is the corresponding critical radius, with $R^* = (\mu \mathrm{Re}^*/\rho\omega)^{0.5}$. μ is the viscosity of air or air-oil mixture.

The dimensionless coefficient C_t is associated with the gear geometry, expressed as:

$$C_t = \xi\frac{z-\varepsilon_a}{4}\frac{b}{r_p}\left[1+\frac{2(1+x_a)}{z}\right]^4(1-\cos\phi)(1+\cos\phi)^3 \tag{8}$$

in which

$$\phi = \pi/z - 2(inv\alpha_p - inv\alpha_a) \tag{9}$$

And

$$\varepsilon_a = [z_1(\tan\alpha_{a1} - \tan\alpha') + z_2(\tan\alpha_{a2} - \tan\alpha')]/(2\pi) \tag{10}$$

where ξ is the reduction coefficient, representing the influence of shrouds, deflectors or casings on the windage losses of the teeth parts. x_a denotes the tooth form coefficient. ε_a is the contact ratio and overlap ratio. α_a, α' are the pressure angle at the addendum and pitch radius, respectively. (z-ε_a) denotes the number of teeth generating the windage losses, after eliminating the teeth that participated in gear engagement.

2.2.2. Pumping losses

As a shroud approaches the spur gear pair, the whole of the gears and the shroud can be regarded as a gear pump. The behavior of pumping fluid through the clearance gap on the top of the tight shroud is similar to the operation principle of a gear. Following the definition of swept volume as described in Ref.[4,42], the squeezing/pocketing losses of the meshed spur gears are expressed as:

$$P_{pump} = \rho\frac{(C_d Q_{mean})^3}{A_s^2} \tag{11}$$

where Q_{mean} is the mean swept volume:

$$Q_{mean} = \frac{b\omega_1}{4}\left[2r_{a1}^2 + 2r_{a2}^2\frac{r_{p1}}{r_{p2}} - 2r_{p1}(r_{p1}+r_{p2}) - \left(1-\frac{r_{p1}}{r_{p2}}\right)l_s^2\right] \tag{12}$$

with l_s denotes the length of the contact line of the meshed gears:

$$l_s = \left(r_{a1}^2 - r_{b1}^2\right)^{0.5} + \left(r_{a2}^2 - r_{b2}^2\right)^{0.5} - (r_{p1}+r_{p2})\sin\alpha \tag{13}$$

where C_d is the discharged coefficient, the orifice flow coefficient equation [43] is the function of the diameter ratio β and Reynolds number Re_{D_h}, then:

$$C_d = 0.5959 + 0.312\beta^{2.1} - 0.184\beta^8 + 0.039\left(\frac{\beta^4}{1-\beta^4}\right) - 0.0337\left(\frac{\beta^3}{w_a}\right) + 0.0029\beta^{2.5}\left(\frac{10^6}{\mathrm{Re}_{D_h}}\right)^{0.75} \tag{14}$$

In this paper, the characteristics ratio of the orifice width w_o to the approach width w_a instead of the diameter ratio is determined as:

$$\beta = \frac{w_o}{w_a} \tag{15}$$

and

$$\mathrm{Re}_{D_h} = \frac{\rho P Q_{mean}}{\pi\mu A_h} \tag{16}$$

P is the wetted perimeter of the orifice, then:

$$P = 2(w_o + l_a) \tag{17}$$

Table 1
Main parameters of the spur gear pair.

Parameter	Pinion 1	Gear 2
Teeth number (z)	44	52
Module (m)	6.35 mm	
Gear width (b)	28.4 mm	
Pressure angle (α_p)	25°	

with l_a is the axial distance of the tight shroud.

A_h is the area of the hydraulic diameter, as the product of the width w_a and distance l_a:

$$A_h = w_a l_a \tag{18}$$

A_s is the area of top clearance of the tight shroud, as the product of the width w_o and distance l_a:

$$A_s = w_o l_a \tag{19}$$

Additionally, as for the mixture of air and oil, the fluid density and viscosity are defined as:

$$\rho = \alpha_{am}\rho_{air} + (1-\alpha_{am})\rho_{oil} \tag{20}$$

and

$$\mu = \alpha_{am}\mu_{air} + (1-\alpha_{am})\mu_{oil} \tag{21}$$

with α_{am} being the volume ratio of air to the total mixture.

3. Test description

The load-independent power loss tests by Hurrell et al [4] were performed on the gear windage test facility of NASA Glenn Research Center, the experimental power losses of the tight shrouded gears were used to compare with the predictions in this paper. The experimental scheme is described in details as follows. The meshed spur gear tests were respectively run in unshrouded and shrouded configurations at the same oil supply conditions. Each test typically involves three steps: progressive acceleration to the preset velocity, hold for tens of seconds, and then start to coast down. This process of test was repeated for a total of three cycles. Meanwhile, the speed-time curves of the gears were recorded to calculate the power losses at different configurations. The pumping and windage losses were finally obtained by a separation method. More details of the gear test apparatus can be found in Ref. [4,27–28]. The spur gear pair (main parameters are listed in Table 1) was tested under the condition of an air-oil mixture with the

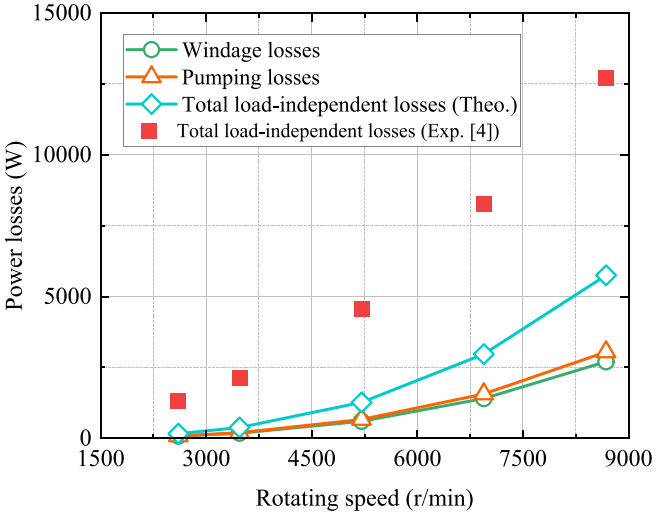

Fig. 3. Comparison of theoretical and experimental load-independent losses for tightly shrouded meshed gears in G1 configuration.

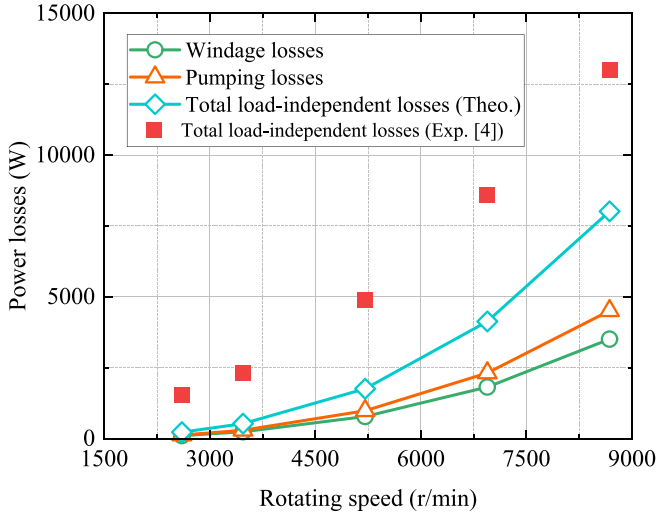

Fig. 4. Comparison of theoretical and experimental load-independent losses for shrouded meshed gears in G2 configuration.

volume ration α_{am} of 0.998 at 38 °C. The axial clearance is 1 mm. The orifice and approach width are 5.44 mm and 5.74 mm for the radial clearance between the pinion or the gear and the shroud is 1 mm, simply as group G1. The orifice and approach width are 3.91 mm and 26.4 mm for the radial clearance is 17 mm, simply as group G2. The rotating speed of the pinion was changed from 0 to about 8700 r/min.

4. Results and discussion

For the tightly shrouded gears, the total load-independent power losses are the sum of the windage losses and the pumping losses. According to Hurrell et. al [4], the windage loss was reduced to 2.7 kW and 3.5 kW for groups G1 and G2 at 8681 r/min (25000 ft/min). The reduction coefficient of windage drag losses in Eq. (8) is achieved as 0.091 for group G1, and 0.131 for group G2. Integrating the reduction coefficient into the windage losses and pumping losses formulas, the total resulting load-independent losses is obtained against the rotating speed and compared with the experimental findings, as shown in Fig. 3 and Fig. 4.

According to the characteristics of the curves in the above figures, there is a great difference between the real experimental load-independent power losses and the anticipated value in theory. In other words, the theoretical prediction method derived from the swept volume of the gear pump already does not apply to the power losses caused by the squeezing/pocketing behavior of the tooth space. There are three big reasons to explain the clear differences. Firstly, the fluid filled with the tooth space is gas (i.e., air or air-oil mixture) instead of liquid, the compressibility of air or air-oil mixture cannot be ignored, especially for the processes of the single-teeth meshing and double-teeth meshing. Secondly, the fluid flow would be changed from subsonic incompressible flow to subsonic compressible flow once the rotating speed exceeds 25,000 ft/min (8681 r/min), where the Mach number is 0.374 over the threshold value of 0.3. Last but not least, the discharge capacity of the tightly shrouded meshed gears in the G1 configuration mainly comes from the teeth spaces, while some swept volume of the shrouded gears in G2 is from the radial clearance of 17 mm. Therefore, these reasons need to be one-by-one analyzed.

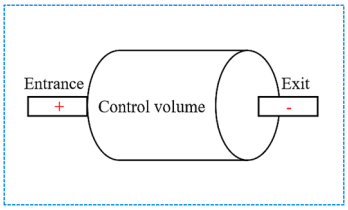

Fig. 5. Open system.

Based on the idea of Seetharaman and Kahraman [6], the influences of air ingestion and discharge at moderate rotating speeds will change the nature of the analysis from incompressible to compressible flow. An assumption is put forward that the changes in air-oil mixture density are caused by the effects of the variations in the volume of the tooth space and the gas ingestion and discharge at low or moderate speeds, while at high speeds of tangential linear speed over subsonic speed the changes of density come from the volumetric change.

For a given tooth space, it is regarded as an open system (Fig. 5), delimited by the pinion and gear surfaces, deformable varying with the rotating angle, and having at least one opening allowing a transfer of air-oil mixture. By convention, the mass flow rate is positive when the fluid enters the open system and negative when it exits. The continuity equation for an open tooth space is:

$$\frac{d}{dt}\iiint_{volume}\rho' dV = \sum_{i=1,n}\iint_{S_i}(\rho\vec{u_i}dS_i\cdot\vec{n_i}) \tag{22}$$

where ρ, ρ' is the density of air-oil mixture outside and in open tooth space, respectively. $\vec{u_i}$ is the velocity vector of the fluid entering or leaving the system, $\vec{n_i}$ is the unit normal at the surface of the fluid outlets & inlets. Eq. (22) is further simplified:

$$\rho' V = \rho V_0 + \rho\pi m z n b[Sr(i-1,j) - Sr(i,j)] \tag{23}$$

where S_r (i,j), S_r $(i\text{-}1,j)$ is the minimum distance between the pinion and gear profiles at the inlet and outlet of the given tooth space. V_0 is the initial volume of tooth space. V is the real-time volume, as the product of the cross-sectional area S_a (i,j) and the gear width b. The changing rate of the tooth space concerning the rotating angle is obtained as:

$$\frac{dV(i,j)}{d\theta} = \frac{V(i,j)^{(\theta+\Delta\theta)} - V(i,j)^{(\theta)}}{\Delta\theta} \tag{24}$$

Based on the profile function of the given tooth in Eq. (3) and (4), the minimum distance, cross-sectional area, volume and the changing rate of volume concerning the rotating angle are determined by leveraging MATLAB, as depicted in Fig. 6 and Fig. 7.

From these changing curves, the minimum distance at the outlet of the tooth space changes to be zero when the root of the pinion tooth

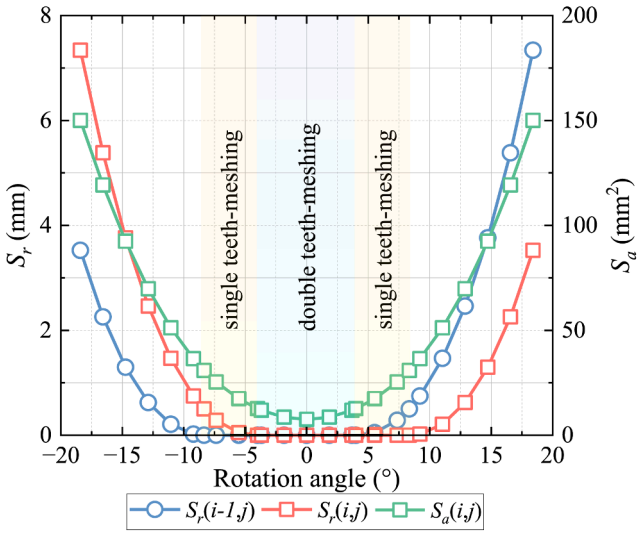

Fig. 6. Minimum distances at the inlet/outlet of the given tooth space and cross-sectional area depending on the rotating angle for a complete compression-expansion phase.

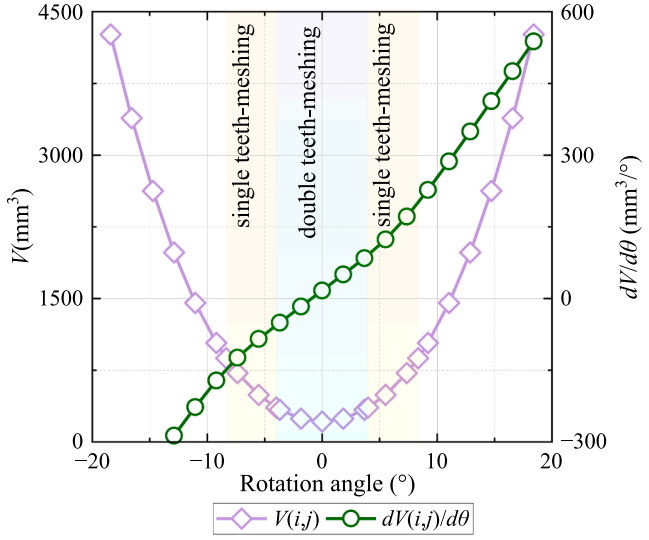

Fig. 7. Volume and its changing rate concerning rotating angle depending on the rotating angle for a complete compression-expansion phase.

contacts with the top of the gear tooth where the single teeth-meshing starts, while the minimum distance at the and intel/outlet is zero when the space is during the double teeth-meshing process. The integral mean values for the minimum distances, cross-sectional area and tooth space volume are adopted and applied to Eq. (23), and the quantity proportion relationship between the mean density and the initial density of the air-oil mixture is obtained. Meanwhile, considering the number of teeth engaged simultaneously, the mean density needs to be multiplied by the contact ratio in Eq. (10).

Following the above assumption, a simplified mean density for predicting the pumping losses will be regarded as a constant at both low and high rotating speed ($n \leq 2000$ r/min, $\rho'_{avg} = 6.98$ kg/m^3; $n \geq 8000$ r/min,$\rho'_{avg} = 3.07$ kg/m^3), with a linear transition at medium speed.

Additionally, the effects of the high tangential speed exceeding 102 m/s at standard atmospheric pressure (Mach number is greater than 0.3) will change the nature of the analysis from subsonic incompressible to subsonic compressible flow. The fluid density for predicting the windage and pumping losses will decrease, expressed as:

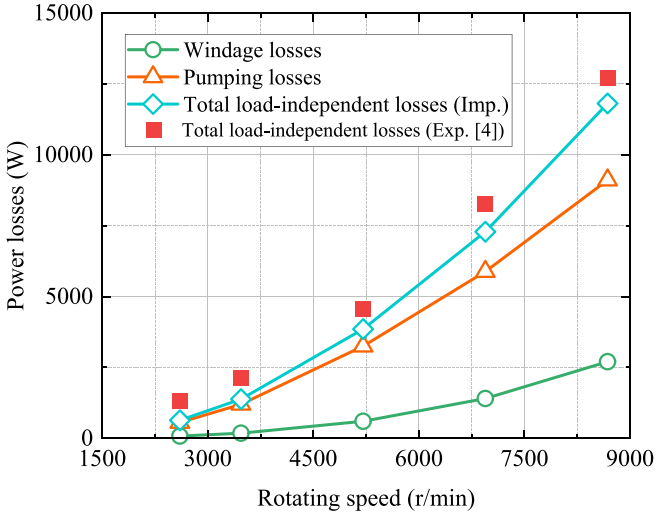

Fig. 8. Comparison of improved theoretical and experimental losses for tightly shrouded meshed gears in G1 configuration.

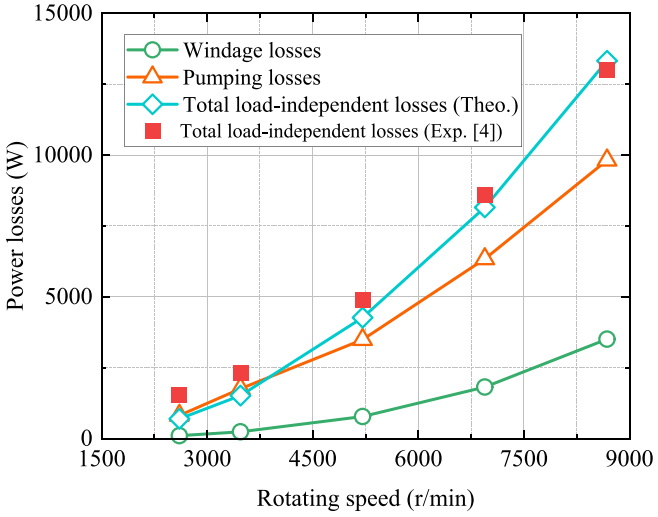

Fig. 9. Comparison of improved theoretical and experimental losses for shrouded meshed gears in G2 configuration.

$$\frac{\rho''}{\rho} = \left(1 + \frac{\gamma - 1}{2} M^2\right)^{-1/(\gamma-1)} \tag{25}$$

where γ is gas constant, $\gamma = 1.4$. M is the Mach number, which is the ratio of the fluid velocity to the sound velocity (sound velocity is 340 m/s at standard atmospheric pressure and 15 °C).

Furthermore, following Fondelli et. al. [36], the velocity of the airflow close to the gear top is about 90 % of the pitch line velocity of the gear. It can also be interpreted as that 90 % of the gas volume surrounding the rotating gears for the relatively loose shroud in G2 configuration, is accelerated and sucked into the tooth space. For this case, the swept volume needs to be multiplied by a correction coefficient of 0.9 in Eq. (11).

Integrating these three factors into Eq. (5), (6) and (11), the improved theoretical analytical model of the total load-independent losses for the tightly shrouded meshed gears is finally determined. Then, different kinds of power losses are calculated and compared with experimental values, as depicted in Fig. 8 and Fig. 9. Clearly, the predictions calculated by the improved theoretical method agree well with experimental results, it is indicated that the method is correct and effective. It is also suggested that the quasi-analytical method is capable of predicting the load-independent power losses for the tightly shrouded meshed gears, especially for the shroud that approaches the gears in axial directions.

Meanwhile, the windage losses and pumping losses at different rotating speeds are also illustrated by using the improved analytical model in Fig. 10. Obviously, more than 75 % of the total load-independent losses are from pumping losses, and the contribution of the pumping losses to the total losses is far greater than that of the windage losses in the same configuration at the same rotating speed. As for the different configurations, the proportion of the pumping losses in G1 is slightly larger than that in G2, it is suggested that a tight shroud makes the behavior of the tightly shrouded gears more similar to the gear pump, with better prediction accuracy. When the rotating speed is advanced, the ratio of the pumping losses slightly decreases and that of the windage losses slightly increases, this shows that the windage loss is more sensitive to the rotating speed. In particular, the total load-independent power losses are about 7.5 kW at the rotating speed of 6944 r/min, and 13 kW at the rotating speed of 8681 r/min. This implies that load-independent power losses can be a major source of power losses at high-speed conditions, especially for pumping losses. It is worth pointing out that this theoretical calculation results for each group can be obtained in a few minutes on an ordinary PC (12th Gen Intel(R) Core

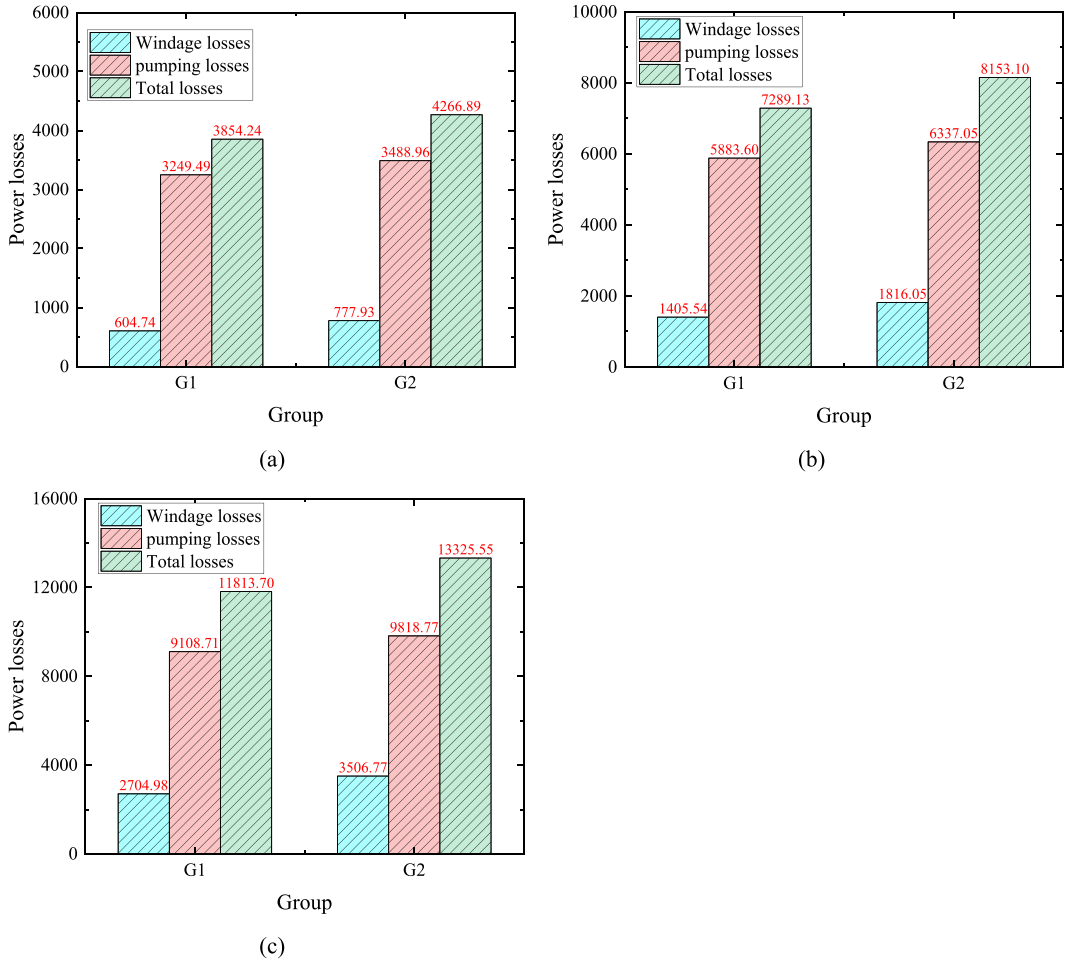

Fig. 10. Distribution of windage and pumping losses against rotating speed for G1 and G2 configurations: a) 5208 r/min; b) 6944 r/min; c) 8681 r/min.

(TM) i7-12700 2.10 GHz), far less time than the experimental or numerical methods.

5. Conclusion

Aiming to explore and predict the load-independent power losses mainly including windage power losses and pumping power losses of a shrouded meshed gear pair, a quasi-analytical method based on the concept of the swept volume for the gear pump is established in this paper, avoiding the disadvantages of high cost for experimental investigations and heavy computation for numerical simulations. The correctness and effectiveness of the theoretical model are verified by comparing it with experiments in open literature. Some conclusions are obtained as follows:

Leveraging the swept volume of the gear pump, the squeezing/pocketing behavior of the air or air-oil mixture in the tooth space of the tightly shrouded meshed gear pair is investigated, thereby the total load-independent power losses are predicted considering the windage and pumping effects. Based on the compressibility of the various in tooth space and subsonic compressible flow, the quasi-analytical model of the total power losses is improved, it is capable of estimating the total losses including the pumping and windage losses, from low speed to high speed. Furthermore, when the pitch line velocity exceeds 127 m/s (8681 r/min), the pumping losses are over 11.3 kW, and it has been a significant contribution to the total power losses.

However, the quasi-analytical method in this paper is limited to predicting the load-independent losses of the tightly shrouded meshed gears that the gear pair is enclosed with the smallest axial and radial clearances. The range of applications needs to be concerned and extended in follow-up studies. Furthermore, the end face and circumferential sealing of the gear device is significantly worse than that of the gear pump system. The leakage of the lubricating medium is not negligible. These factors do have an impact on the model computation precision, especially in the case of a larger clearance between the gears and the shroud. Follow-up studies of this pumping loss model are being planned from two aspects: on the one hand, the influence of the air flow at the import and export of tight shrouded gear pair needs further investigated; on the other hand, The leakage of the lubricating medium at the end face should be focused.

Declaration of Competing Interest

The authors declare that they have no known competing financial interests or personal relationships that could have appeared to influence the work reported in this paper.

Acknowledgments

The authors are deeply grateful for the funding from the National Natural Science Foundation of China (Grant No. 52305081), Natural Science Foundation of Changsha City of China (Grant No. kq2208275), and the National Defense Pre-Research Foundation of China (Grant No. KY-44-2018-0219).

References

[1] R. Handschuh, C. Kilmain, Operational influence on thermal behavior of high-speed helical gear trains, AHS International 62nd Annual Forum and Technology Display; Phoenix, Arizona, May 9–11, 2006. Paper No. NASA/TM-2006-214344.

[2] T.T. Petry-Johnson, P. Johnson, A. Kahraman, N.E. Anderson, D.R. Chase, An experimental investigation of spur gear efficiency, J. Mech. Des. 130 (2008), https://doi.org/10.1115/1.2898876.

[3] R. Handschuh, C. Kilmain, Preliminary comparison of experimental and analytical efficiency results of high-speed helical gear trains, In: ASME 2003 international design engineering technical conferences and computers and information in engineering conference; Chicago, Illinois, USA, 2-6 September, 2003. https://doi.org/10.1115/DETC2003/PTG-48116.

[4] M.J. Hurrell, J.T. Sawicki, Pumping Loss of Shrouded Meshed Spur Gears, J. Eng. Gas Turb. Power 142 (11) (2020), 111003, https://doi.org/10.1115/1.4048487.

[5] H. Arisawa, M. Nishimura, H. Imai, T. Goi, CFD simulation for reduction of oil churning loss and windage loss on aeroengine transmission gears, In Turbo Expo: Power for Land, Sea, and Air 48821 (2009) 63–72, https://doi.org/10.1115/GT2009-59226.

[6] Y. Diab, F. Ville, P. Velex, C. Changenet, Windage losses in high speed gears preliminary: experimental and theoretical results, J. Mech. Des. Trans. ASME 126 (2004) 903–908, https://doi.org/10.1115/1.1767815.

[7] S. Seetharaman, A. Kahraman, Load-independent spin power losses of a spur gear pair: model formulation, J. Tribol. ASME 131 (2009), https://doi.org/10.1115/1.3085943.

[8] S. Seetharaman, A. Kahraman, A windage power loss model for spur gear pairs, Tribol. t. 53 (4) (2010) 473–484, https://doi.org/10.1080/10402000903452848.

[9] S. Seetharaman, A. Kahraman, M.D. Moorhead, et al., Oil churning power losses of a gear pair: experiments and model validation, J. Tribol. ASME 131 (2) (2009), 022202, https://doi.org/10.1115/1.3085942.

[10] X. Zhu, Y. Dai Y, FY. Ma, Development of a quasi-analytical model to predict the windage power losses of a spiral bevel gear, Tribol. Int. 146 2020 106258. https://doi.org/10.1016/j.triboint.2020.106258.

[11] X. Zhu, Y. Dai, F.Y. Ma, On the estimation of the windage power losses of spiral bevel gears: An analytical model and CFD investigation, Simul. Model. Pract. Th. 110 (2021), 102334, https://doi.org/10.1016/j.simpat.2021.102334.

[12] M. Ruzek, F. Ville, P. Velex, et al., On windage losses in high-speed pinion-gear pairs, Mech. Mach. Theor. 132 (2019) 123–132, https://doi.org/10.1016/j.mechmachtheory.2018.10.018.

[13] M. Ruzek, Y. Marchesse, F. Ville, et al., Windage power loss reductions in high-speed gear pairs, Forsch. Im. Ingenieurwes 83 (3) (2019) 387–392, https://doi.org/10.1007/s10010-019-00336-7.

[14] Y. Dai, L. Xu, X. Zhu, et al., Application of an unstructured overset method for predicting the gear windage power losses, Eng. Appl. Comp. Fluid 15 (1) (2021) 130–141, https://doi.org/10.1080/19942060.2020.1858166.

[15] S. Laruelle, C. Fossier, C. Changenet, F. Ville, S. Koechlin, Experimental investigations and analysis on churning losses of splash lubricated spiral bevel gears, Mec, Ind. 18 (4) (2017), https://doi.org/10.1051/meca/2017007.

[16] R. Quiban, C. Changenet, Y. Marchesse, F. Ville, J. Belmonte, Churning losses of spiral bevel gears at high rotational speed, Proc. IME. J J. Eng. Tribol. 234 (2) (2020) 172–182, https://doi.org/10.1177/1350650119858236.

[17] Y. Dai, F. Ma, X. Zhu, et al., Development of a quasi-analytical model to predict the windage power losses of a spiral bevel gear, Tribol. Int. 151 (2020), 106536, https://doi.org/10.1016/j.triboint.2020.106536.

[18] Y. Dai, X. Chen, D. Yang, et al., Impulse power loss in orthogonal face gear–numerical and experimental results, Eur. Phys. J. plus 138 (1) (2023) 88, https://doi.org/10.1140/epjp/s13360-023-03653-7.

[19] X. Zhu, Y. Dai, Development of an analytical model to predict the churning power losses of an orthogonal face gear, Eng. Sci. Technol. (2023), https://doi.org/10.1016/j.jestch.2023.101383. In press.

[20] E. Hartono, M. Golubev, V. Chernoray, PIV study of fluid flow inside a gearbox, Tenth International Symposium on Particle Image Velocimetry, Delft, The Netherlands, July 1–3, 2013. Paper No. PIV13.

[21] E. A. Hartono, A. Pavlenko, V. Chernoray, Stereo-PIV study of oil flow inside a model gearbox, 17th International Symposium on Applications of Laser Techniques to Fluid Mechanics. Lisbon, Portugal, July 7–10, 2014.pp. 1–8.

[22] N. Voeltzel, Y. Marchesse, C. Changenet, et al., On the influence of helix angle and face width on gear windage losses, P. i. Mech. Eng. C-J. Mec. 230 (7–8) (2016) 1101–1112, https://doi.org/10.1177/0954406215602036.

[23] E. Burberi, T. Fondelli, A. Andreini, et al, CFD simulations of a meshing gear pair. Turbo Expo: Power for Land, Sea, and Air, American Society of Mechanical Engineers. Seoul, South Korea, June 13–17, 2016. V05AT15A024. https://doi.org/10.1115/GT2016-57454.

[24] Y. Diab, F. Ville, H. Houjoh, et al., Experimental and numerical investigations on the air-pumping phenomenon in high-speed spur and helical gears, P. i. Mech. Eng. C-J. Mec. 219 (8) (2005) 785–800, https://doi.org/10.1243/095440605X31652.

[25] D. Talbot, A. Kahraman, S. Seetharaman, A helical gear pair pocketing power loss model, J. Tribol.-t. ASME 136 (2) (2014), 021105, https://doi.org/10.1115/1.4026502.

[26] C. Gorla, F. Concli, K. Stahl, et al., Hydraulic losses of a gearbox: CFD analysis and experiments, Tribol. Int. 66 (2013) 337–344, https://doi.org/10.1016/j.triboint.2013.06.005.

[27] I. Delgado, M. Hurrell, The effectiveness of shrouding on reducing meshed spur gear power loss—test results, AGMA Fall Technical Meeting, Columbus, OH, Oct. 22–24, 2017. Paper No. 17FTM04.

[28] M. J. Hurrell, I. Delgado, J. T. Sawicki, Swept volume approach for the characterization of pumping loss of shrouded meshed cylindrical gears, Annual Forum and Technology Display. 2019 (GRC-E-DAA-TN67693).

[29] Bakırcı, M., & Yılmaz, S. (2018). Theoretical and computational investigations of the optimal tip-speed ratio of horizontal-axis wind turbines, Eng Sci Technol. 21(6) (2018) 1128-1142. https://doi.org/10.1016/j.jestch.2018.05.006.

[30] M. Daş, E. Alıç, E.K. Akpinar, Numerical and experimental analysis of heat and mass transfer in the drying process of the solar drying system, Eng. Sci. Technol. 24 (1) (2021) 236–246, https://doi.org/10.1016/j.jestch.2020.10.003.

[31] T.T. Devi, B. Kumar, Mass transfer and power characteristics of stirred tank with Rushton and curved blade impeller, Eng. Sci. Technol. 20 (2) (2017) 730–737, https://doi.org/10.1016/j.jestch.2016.11.005.

[32] F. Concli, C. Gorla, A. Della Torre, et al, Windage power losses of ordinary gears: different CFD approaches aimed to the reduction of the computational effort, Lubricants 2(4) 2014 162–76. https://doi.org/10.3390/lubricants2040162.

[33] F. Concli, C. Gorla, Numerical modeling of the power losses in geared transmissions: windage, churning and cavitation simulations with a new integrated approach that drastically reduces the computational effort, Tribol. Int. 103 (2016) 58–68, https://doi.org/10.1016/j.triboint.2016.06.046.

[34] F. Concli, T.A. Della, C. Gorla, G. Montenegro, A new integrated approach for the prediction of the load independent power losses of gears: development of a mesh handling algorithm to reduce the CFD simulation time, Adv. Tribol. (2016) 1–6, https://doi.org/10.1155/2016/2957151.

[35] F. Concli, C. Gorla, Numerical modeling of the churning power losses in planetary gearboxes: an innovative partitioning based meshing methodology for the application of a computational effort reduction strategy to complex gearbox configurations, Lubric. Sci. 29 (7) (2017) 455–474, https://doi.org/10.1002/ls.1380.

[36] F. Concli, C. Gorla, Computational and experimental analysis of the churning power losses in an industrial planetary speed reducer, WIT Trans. Eng. Sci. 74 (2012) 287–298, https://doi.org/10.2495/AFM120261.

[37] H. Liu, T. Jurkschat, T. Lohner, K. Stahl, Determination of oil distribution and churning power loss of gearboxes by finite volume CFD method, Tribol. Int. 109 (2017) 346–354, https://doi.org/10.1016/j.triboint.2016.12.042.

[38] X.Z. Hu, Y.Y. Jiang, C. Luo, L.F. Feng, Y. Dai, Churning power losses of a gearbox with spiral bevel geared transmission, Tribol. Int. 129 (2019) 398–406, https://doi.org/10.1016/j.triboint.2018.08.041.

[39] T. Fondelli, A. Andreini, R. Da Soghe, et al., Numerical simulation of oil jet lubrication for high speed gears, Int. J. Aerosp. Eng. 2015 (2015), https://doi.org/10.1155/2015/752457.

[40] D. Massini, T. Fondelli, B. Facchini, et al, Experimental investigation on power losses due to oil jet lubrication in high speed gearing systems. in Proceedings of the ASME turbo expo 2017: turbomachinery technical conference and exposition. Heat Transfer, Charlotte, vol. 50886 (2017). https://doi.org/10.1115/GT2017-64703.

[41] B. C. Al, K. Simmons, H. P. Morvan , Computational investigation of flows and pressure fields associated with spur gear meshing, Turbo Expo: Power for Land, Sea, and Air. American Society of Mechanical Engineers. Düsseldorf, Germany, June 16–20, 2014.: V05CT16A023. https://doi.org/10.1115/GT2014-26145.

[42] N.D. Manring, S.B. Kasaragadda, The theoretical flow ripple of an external gear pump, J. Dyn. Sys., Meas. Control 125(3) 2003 396-404. https://doi.org/10.1115/1.1592193.

[43] Orifice Flow Coefficient Equation Comparison. ASME STP-TS-084-2018. 2018.